JOURNAL OF MATERIALS SCIENCE 16 (1981) 3371–3380

Influence of processing conditions on the structure and surface microhardness of injection-moulded polyethylene

D. R. RUEDA, F. J. BALTÁ CALLEJA
Instituto de Estructura de la Materia, CSIC, Madrid 6, Spain

R. K. BAYER
Institut für Werkstofftechnik, Universität Gesamthochschule, Kassel, West Germany

Linear polyethylene (PE) was injection-moulded into standard tensile bars using a range of melt, T_s, and mould, T_w, temperatures. Microhardness testing and X-ray small- and wide-angle diffraction techniques were used to investigate the changes in mechanical properties, microstructure and crystalline orientation, occurring throughout the range of mouldings. A correlation was shown to exist between microstructure and processing variables. Thus, a clear increase in hardness anisotropy, ΔMH, (from 15 up to about 30%), corresponding to a well-developed molecular and lamellar orientation, and hardening (for high molecular grade PE), especially when decreasing the melt temperature below 200° C, has been detected. This increase in ΔMH favours the view of an increase of a substantial fraction of tie molecules contributing to the local instant elastic recovery beneath the indenter along the injection direction. ΔMH is, however, nearly independent of T_s for conventional moulding-grade PE. Here the absence of a unit-cell orientation is evident in the T_s range investigated while a lamellar orientation only prevails for $T_s < 200°$ C. In this latter case $MH_\perp$ is a linear function of T_w. This result is consistent with the fact that microhardness increases with the fraction of crystallized material. The obtained results suggest that the three-dimensional molecular network existing in the material plays a relevant role in steering the mechanical behaviour of the final lamellar moulded material.

1. Introduction

In the last few years the study of microhardness of semi-crystalline polymers, particularly polyethylene (PE), has been the subject of an extensive research program in this laboratory. In previous papers [1–5] we have shown that microhardness is extremely sensitive to the morphological and textural changes undergone by polymeric materials. This is due to the fact that indentation-hardness is based on plastic straining and eventually on elastic release and, hence, is intimately correlated to the intervening molecular and supermolecular deformation mechanisms occurring in polymers. These include crystalline phase changes, molecular shear within the crystallites, interlamellar shear, block fracture, etc. [6]. The prevailing deformation mechanism finally depends on the specific morphology of the material. In isotropic melt-crystallized PE during cooling, the microhardness is primarily an increasing function of crystal thickness and depends, in addition, on the fraction of crystalline material [1]. The thicker are the crystals (hard elements), the higher is the cohesion energy, opposing, as a result, a greater resistance to plastic deformation. The interlamellar non-crystalline component and lateral grain boundaries contribute, on the other hand, to a lowering of the hardness value. Recent studies on isothermally-crystallized lamellar PE emphasize the fact that hardness is dependent on the packing density of molecules within the crystalline and non-crystalline regions [5]. As a result, the overall hardness of the

0022–2461/81/123371–10$03.00/0

material is an increasing function of the macroscopic density. Concerning the micromechanical properties of the crystallites themselves, the microhardness of the crystalline regions of the material has, furthermore, been shown to be related to the molecular cross-section of the crystal unit-cell [7]. The crystallite hardness is, in addition, an increasing function of the crystal thickness and coherently-diffracting lattice volume [5].

Microhardness, *MH*, is also a very useful property, providing a direct measure of the anisotropy developed within fibres and highly drawn polymers. The hardness anisotropy, ΔMH, is a consequence of the high orientation of molecular chains coupled with, on unloading, preferential local elastic recovery of the material, along the chain direction. In oriented chain-extended PE with a given draw-ratio, the microhardness is found to be a function of annealing temperature and, consequently, of chain extension [2]. In the case of ultra-oriented PE, microhardness has been shown to increase with both pressure and temperature of extrusion [4]. The hardening of the material has been ascribed to an improvement in the strength and lateral packing of fibrils and microfibrils in the fibre direction. In these highly oriented systems, ΔMH, which offers a measure of preferred chain-axis orientation, was shown to be a function of draw-ratio. This is, in fact, a very important result since it permits a correlation to be drawn between ΔMH and the longitudinal elastic modulus and, hence, the number of tie molecules.

It is known, that process variables in injection moulding provoke substantial changes in the microstructure of the moulded material. Variations often occur in the plane surfaces and across the thicknesses of flat samples [8]; as a result, the mechanical properties are governed by different variables such as melt temperature, ageing, mould packing and thickness [9–11]. In a recent study, it has been shown that the processing conditions of injection-moulded PE strongly influence physical properties such as elastic modulus, macroscopic density, yield point, shrinkage and breaking strength [12, 13]. The purpose of the present study is, hence, to relate some of the process variables to microstructure details of injection-moulded PE by means of a combined microhardness and X-ray diffraction pattern study. The microhardness test has been previously utilized with success for the investigation of the microstructure of injection-moulded TPX, an ICI commercial thermoplastic [14, 15]. The great advantage of this method lies in the simplicity and rapidity of experiments and in the fact that the tested samples remain unaltered [indentations are localized in a small volume element ($\sim 10^{11}$ nm^3)]. In this paper the results of *MH* experiments performed on the surface of the PE mouldings will be described. In a forthcoming study, additional information concerning the *MH* variations occurring across the moulding thickness will be also reported. Since molecular weight is a variable which strongly influences the elastic properties of the melt [16] attention in this work has been concentrated on two types of samples substantially differing in molecular weight. The elastic properties are, in turn, steering the structure of the already pre-existing molecular network in the molten polymer [12, 16]. The concept of a network has been very helpful in understanding the drawing behaviour of polymers [17–19]. The elasticity of the melt can be changed during the injection-moulding process by adequately varying the molecular weight and the temperature of the molten polymer. It is wished, therefore, to raise also the question of whether study of the microhardness, and its dependence on the above processing variables, can yield valid conclusions concerning the molecular network structure which embodies both the crystalline and non-crystalline material.

2. Experimental procedure

2.1. Materials and processing conditions

Lupolen 5261-Z, a very high molecular weight grade ($M_w \sim 450\,000$), and Lupolen 6011-L, a typical injection-moulding grade ($\bar{M}_w \sim 100\,000$), were used in this study. These materials in bulk form have a crystalline weight fraction of between 0.7 and 0.75.

The mouldings were prepared in the form of ASTM tensile bars (gauge length 50 mm, thickness 4 mm and width 10 mm) using a Stübbe SKM 51 injection moulder. Fig. 1 shows the relation between the shape and co-ordinates of the bar and the injection direction. The moulding cycle consists of two parts:

(a) a recharge during which the molten polymer, at a temperature T_s, is conveyed under a developed pressure ahead of a rotating screw till sufficient mass is available to be discharged into the mould assembly; and

(b) injection of the melt through the sprue into

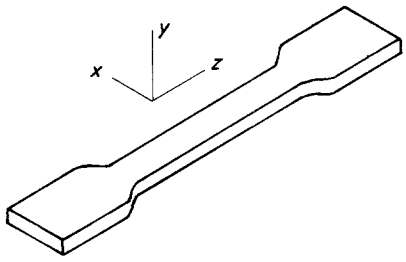

Figure 1 Co-ordinates for the injection-moulded bar: z, injection direction; y, normal to the bar surface; x, orthogonal to y and z. Indentations were made on the bar surface (xz-plane) with one diagonal of the indenter parallel (z) and one perpendicular (x) to the injection direction. The incident X-ray beam was parallel to the y-direction.

the mould cavity where the polymer is formed at the desired temperature, T_w.

The bars were moulded under a range of melt temperatures, T_s, and mould temperatures, T_w, between 140 and 300° C and 25 and 95° C, respectively. The processing conditions were organized according to the four series of the following scheme:

(i) Variation of T_s ($T_w = 45°$ C);
(ii) Variation of T_w (medium $T_s = 240°$ C);
(iii) Variation of T_w (high $T_s = 270°$ C); and
(iv) Variation of T_w (low $T_s = 160°$ C).

The injection pressure was kept constant and equal to 73 MPa. The moulding conditions are given in Tables I and II. Density measurements of the mouldings were made using an isopropanol–water density gradient column. For Lupolen 5261-Z and $T_s > 210°$ C, the time required to recharge the barrel is 9 sec. Then the polymer is stored for a further 19 sec to reach thermal equilibrium at T_s before injection. For $T_s = 270$ and 300° C the time for which the mass was at rest was 9 sec. For $T_s < 210°$ C the screw has difficulty in pushing the highly viscous polymer along the barrel. The mass transport proceeds so slowly that no resting time was left before injection. The recharge time here was 28 sec. For Lupolen 6011-L, resting times of 19 sec were selected. However, high T_s (240 to 340° C) and T_w (85 to 95° C) values require longer cooling periods for the moulding extraction. This led to a time of rest of 33 sec. After a given induction time for the filling operation the mould cavity pressure increases instantly. Values of 48 and 55 MPa were used in the present experiments. Injection takes place rapidly followed by a cooling stage during which the cavity pressure drops, after a time of about 25 sec, to zero at solidification. After injection, the runner to the cavity was frozen to avoid any back-flow of material. The freeze time, t_f, depends strongly on T_s and only

TABLE I Processing conditions, microhardness parallel ($MH_{\parallel}$) and perpendicular ($MH_{\perp}$) to the injection direction and microhardness anisotropy (ΔMH) of Lupolen 5261-Z

T_s (° C)	T_w (° C)	$MH_{\parallel}$ (MN m^{-2})	$MH_{\perp}$ (MN m^{-2})	ΔMH (%)
140	45	93.2	65.2	30.0
160	45	86.0	62.9	26.9
180	45	80.6	59.5	26.2
210	45	67.5	58.1	14.0
240	45	63.4	54.2	14.4
270	45	60.9	52.0	14.7
300	45	58.3	50.6	13.1
340	45	55.8	50.0	11.6
240	25	66.6	57.3	14.0
240	35	60.3	52.2	13.5
240	55	58.5	50.8	13.2
240	70	57.7	50.1	13.1
240	85	68.4	57.6	15.8
240	95	69.1	53.8	22.2
270	95	63.8	57.0	10.6
270	85	68.9	54.8	20.4
270	70	68.2	58.6	14.1
270	55	67.3	58.4	13.3
160	32	96.1	71.5	26.6
160	55	82.5	57.2	30.7
160	25	86.2	59.4	31.1

TABLE II Processing conditions, microhardness parallel ($MH_{\parallel}$) and perpendicular ($MH_{\perp}$) to the injection direction and microhardness anisotropy (ΔMH) of Lupolen 6011-L

T_s (° C)	T_w (° C)	$MH_{\parallel}$ (MN m^{-2})	$MH_{\perp}$ (MN m^{-2})	ΔMH (%)
140	46	55.9	50.1	10.3
160	46	59.0	53.5	9.3
180	46	57.1	51.1	10.5
210	46	51.8	49.5	4.4
240	46	54.6	52.0	4.8
270	46	56.2	51.2	8.9
300	46	62.0	57.2	7.8
340	46	60.0	56.9	5.2
240	26	50.3	50.8	~ 0
240	35	55.3	55.2	~ 0
240	55	54.1	54.0	~ 0
240	70	58.1	57.9	~ 0
240	85	58.1	59.5	~ 0
240	95	62.0	62.1	~ 0
270	95	61.2	63.6	~ 0
270	85	56.6	59.4	~ 0
270	70	59.2	58.6	~ 0
270	55	56.3	55.4	~ 0
160	35	54.3	55.1	~ 0
160	55	56.3	58.3	~ 0
160	26	49.9	50.5	~ 0

slightly on T_w. In any case the time in which the cavity is under pressure was selected to be larger than t_f. The temperature of the mould when extraction takes place is unknown. After cooling down, the mouldings do not reach thermal equilibrium immediately. For Lupolen 5261-Z, for instance, crystallization takes place over one week on storage.

2.2. Micro-indentation hardness measurements

For the micro-indentation experiments surface polishing of the bar surface to a 1 μm diamond paste was used to improve focusing. The microhardness measurements were carried out with a Leitz microhardness tester and a Vickers square pyramidal diamond. The diamond was aligned so that the diagonals were parallel and perpendicular to the injection direction. At least 10 sets of indentations, about 100 μm centre-to-centre apart, were made at room temperature (25° C) along the injection direction (z-axis) on the xz-surface of each sample. A load of 15 g was applied in each case for a time $\tau = t_s + t$ where t_s is the sinking time of the indenter until the moulding surface ($t_s \sim 8$ sec) is reached and t is the actual loading time ($t = 6$ sec). The dimensions of the diagonals of the diamond-shaped indentation were measured immediately after load release so that delayed recovery would be minimized. The elastic recovery of the material was undectable within the experimental error. The hardness value (in MN m^{-2}) was derived using the well-known expression

$$MH = kP/d^2, \quad (1)$$

where d is the length of the indentation diagonal in μm, P is the load applied in g and k is a geometrical factor equal to 1.8191×10^4. Due to the inherent surface inhomogeneity of the mouldings the accuracy of measurements of microhardness is within 5%. Further details of the microhardness measurements and data evaluation have been described in previous publications [1–4].

2.3. X-ray diffraction techniques

The samples were also examined using X-ray diffraction techniques. For this purpose the tensile bars were cut from the surface with a sharp knife in the centre of the bar in the form of parallelepipeds of 10 mm x 0.6 mm x 1.5 mm. Small-angle X-ray diffraction (SAXD) photographs were taken at room temperature with a Rigaku camera and an RU-3 rotary anode tube. Cu$K\alpha$ radiation with a Ni-Filter was used. The photo-

graphs were taken with the beam perpendicular to both the injection direction and the xz-surface of the mouldings. The size of the beam impinging on the sample was about 0.2 mm. The working conditions were 40 kV and 180 mA and a specimen–film distance of 400 mm. The long periods, L, were derived from the position of the first diffraction maxima after background subtraction. Their positions can be estimated to within $\Delta L/L = 3$ to 5×10^{-2}. Wide-angle X-ray diffraction (WAXD) photographs were obtained at room temperature in a flat camera with a specimen–film distance of 40 mm. For the determination of the unit-cell orientation, equi-inclination photographs were also taken.

3. Results

3.1. Dependence of melt temperature

The obtained surface microhardness data for the two investigated series of mouldings are collected in Tables I and II. The most relevant feature of the series of high molecular weight (Lupolen 5261-Z) is the clear anisotropy exhibited by the impressions. The Vickers hardness value is a maximum when the indentation diagonal is parallel with the injection direction, $MH_{\parallel}$, and a minimum when normal to it, $MH_{\perp}$. For the high molecular weight Lupolen 5261-Z, Fig. 2 (solid symbols) shows the gradual decrease of hardness in both directions with increasing T_s (for $T_w = 45°$ C). For the samples of lower molecular weight (Lupolen 6011-L), Fig. 2 (open symbols) shows that the hardness is nearly independent of T_s. Here the samples of the Series i were moulded under a smaller pressure (48 MPa) than those of Series ii to iv (about 55 MPa). This difference in pressure results in lower $MH_{\perp}$ values for Series i, with the exception of the samples for $T_s = 300$ and 340° C. These two samples show the highest $MH_{\perp}$ values (see Table II). This is due to the fact that they were moulded at a pressure of 58 MPa. The hardness anisotropy (in per cent),

$$\Delta MH = MH_{\parallel} - MH_{\perp}, \qquad (2)$$

which first decreases slowly with T_s for Lupolen 5261-Z, shows a sudden decrease in the vicinity of 210° C from $\Delta MH = 27\%$ down to $\Delta MH = 14\%$ (see Fig. 3). Thereafter, ΔMH remains nearly constant. For Lupolen 6011-L the hardness anisotropy values are substantially lower than for Lupolen 5261-Z, showing, also, a tendency to decrease with T_s. Since the penetration depth is nearly the same (9.3 to 10.6 μm) for both polymers, any influence of the depth of penetration on the microhardness data can consequently be discarded in these experiments.

The series of Lupolen 5261-Z moulds yields a two-spot meridional SAXD (Fig. 4) indicating a uniform orientation of relatively perfect lamellae perpendicular to the injection direction. At sufficiently long exposure times a faint second-order reflection can also be observed. The ratio of the heights of the first and second maxima is about 2.2. The obtained long period values are shown in Fig. 4, plotted against T_s. The SAXD pattern for Lupolen 6011-L shows two faint-intensity meridional parallel to the injection direction superposed on a relatively strong uniform ring for samples prepared using melt temperatures up to $T_s = 240°$ C. For $T_s > 240°$ C the SAXD pattern is

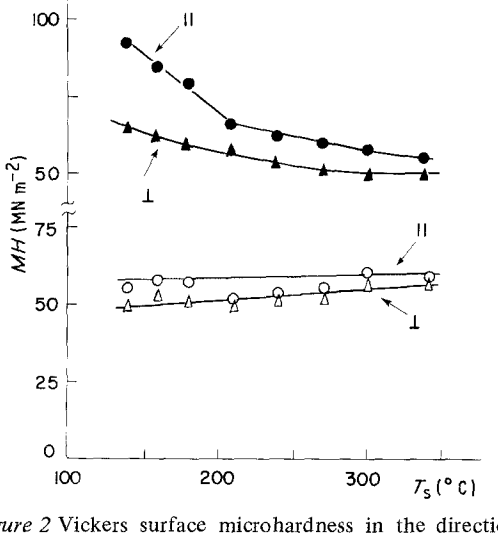

Figure 2 Vickers surface microhardness in the direction parallel (||) and perpendicular (⊥) to the injection direction of injection-moulded PE as a function of melt temperature for high molecular weight grade PE (Lupolen 5261-Z) (closed symbols) and typical injection-moulding grade PE (Lupolen 6011-L) (open symbols). $T_w = 45°$ C.

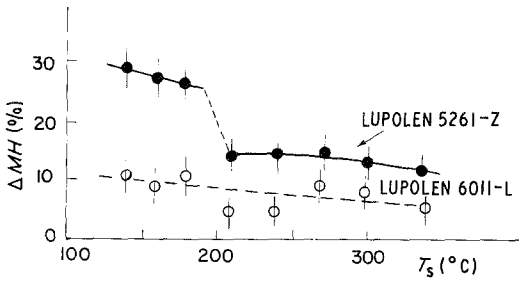

Figure 3 Microhardness anisotropy, at the surface of moulding, as a function of melt temperature in injection moulder for: high molecular grade PE (•) and typical injection-moulding grade (○). $T_w = 45°$ C.

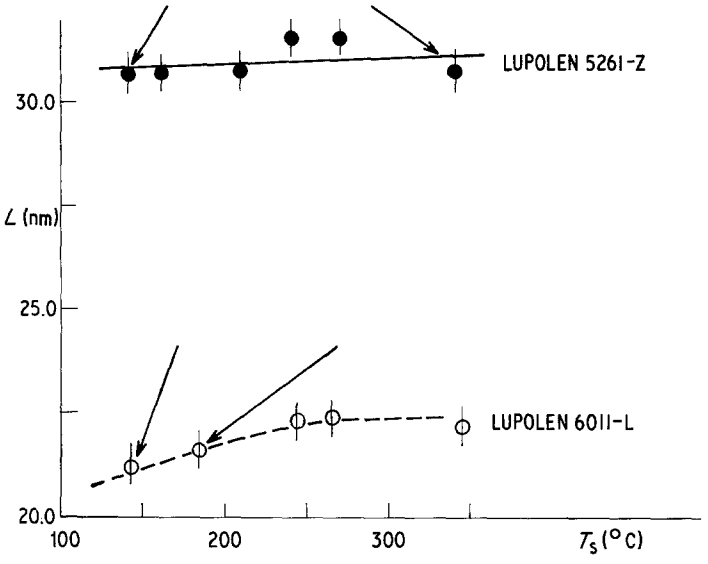

Figure 4 X-ray long period, L, as a function of melt temperature for: high molecular grade PE (•) and typical injection-moulding grade material (○), together with representative SAXD and WAXD photographs. Injection direction: vertical; X-ray beam: parallel to y-direction. The WAXD photograph for Lupolen 5261-Z indicates a c-axis orientation parallel to the z-direction. $T_w = 45°$ C.

simply a ring with no tangential intensity variation. The long period of this series varies only very slightly with increasing T_s, from 21.2 up to 22.0 nm. The WAXD pattern (Fig. 4) for Lupolen 5261-Z shows a relatively well oriented fibre structure with the c-axis parallel to the injection direction. The unit cell orientation remains unaltered with T_s. The WAXD patterns for Lupolen 6011-L show, on the contrary, the presence of isotropic diffraction rings, i.e. complete unit cell disorientation.

3.2. Dependence of mould temperature

Fig. 5 shows, within the observed fluctuation of values, the constancy of $MH_\perp$, for Lupolen 5261-Z, and the slightly linear increase of $MH_\perp$ as a function of increasing mould temperature for Lupolen 6011-L. Fig. 6 illustrates the dependence of hardness anisotropy on T_w for both polymers. For Lupolen 5261-Z, ΔMH is constant in the range $T_w = 25$ to 50° C while it dramatically increases with T_w above 75° C. However, for Lupolen 6011-L, ΔMH is zero for the whole range of T_w temperatures. These differing behaviours of ΔMH for the T_w series and the T_s series (Table II) could be attributed to the above mentioned difference in the mould pressure used in both series. The conspicuous influence of mould temperature on both X-ray long-period, L, and density, ρ, is depicted for the two polymers under study in

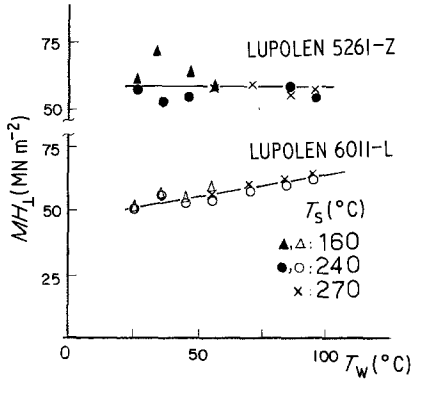

Figure 5 Vickers surface microhardness in the direction perpendicular to the injection direction as a function of temperature in the mould cavity for high molecular weight grade PE (closed symbols) and typical injection-moulding grade PE (open symbols). Melt temperatures are indicated.

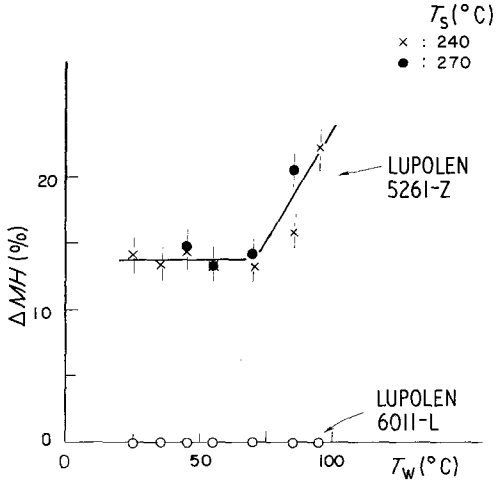

Figure 6 Microhardness anisotropy at the surface as a function of mould temperature for high molecular grade PE (closed symbols) and current injection-moulding grade PE (open symbols).

Figs 7 and 8. Thus, for Lupolen 5261-Z, L linearly increases from $L \sim 30.0$ nm for $T_w = 25°$ C up to $L = 35.0$ nm for $T_w = 95°$ C; for Lupolen 6011-L the L values are approximately a third to a quarter smaller and the increase of L with T_w is half as great. However, while the increase of density, ρ, with T_w is also nearly linear for both polymers (Fig. 8) the density values are approximately 10% lower for the high molecular grade PE. This suggests that for this material the lamellar thickness is larger though the perfection of the crystals is substantially smaller than for the typical injection-moulding grade PE. The plot of ρ against L^{-1} for each series of mouldings (Fig. 9) yields a straight line which can be represented by

$$\rho = \rho_c - A/L, \qquad (3)$$

where the slope A is constant for each polymer and ρ_c is the density of a crystalline lamellae of infinite thickness. This plot is consistent with the concept of a two-phase model of crystalline lamellae and "amorphous" surface layer arrangement where $A = (\rho_c - \rho_a)a$ [20], a is the surface layer thickness and ρ_a is the surface layer density. The constant A and hence a, increases with molecular weight but is independent of lamella thickness. The latter crystal thickness increases with T_w contributing, as a result, to the observed density increase shown in Fig. 8. Assuming a value of the density change, $\Delta\rho \sim 0.16\,\mathrm{g\,cm^{-3}}$ [21] one

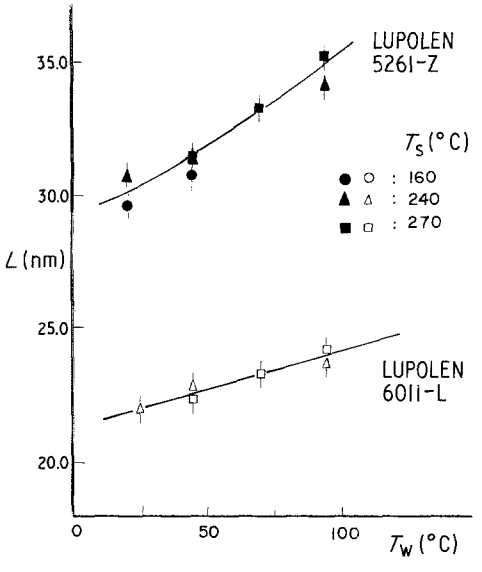

Figure 7 Long period, L, against mould temperature for high molecular grade PE (closed symbols) and conventional injection-moulding grade (open symbols) for different melt temperatures.

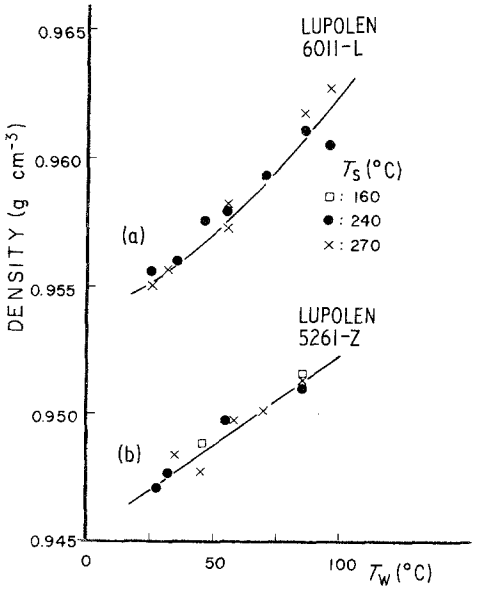

Figure 8 Dependence of the density of (a) typical injection-moulding grade and (b) high molecular grade PE moulding on mould temperature for different melt temperatures.

obtains values for a of 7.0 nm (Lupolen 6011-L) and 12.5 nm (Lupolen 5261-Z), respectively. The intercept of the straight lines on the ordinate axis, $\rho_c = 1.01\,\mathrm{g\,cm^{-3}}$ is close to the accepted values of the crystalline unit-cell density of PE [22]. Finally, the analysis of the integral width of the (1 1 0) reflections indicates that the lateral dimensions, d_{110} of the crystals perpendicular to this direction concurrently increase with increasing T_w. For Lupolen 5261-Z, for instance, d_{110} decreases from 48.7 nm for $T_w = 25°$ C up to 56.7 nm for $T_w = 95°$ C. The paracrystalline lattice distortions, g, are here of the order of $g_{110} = 0.8\%$ and apparently, within the error of experiment, remain unaltered with increase of T_w.

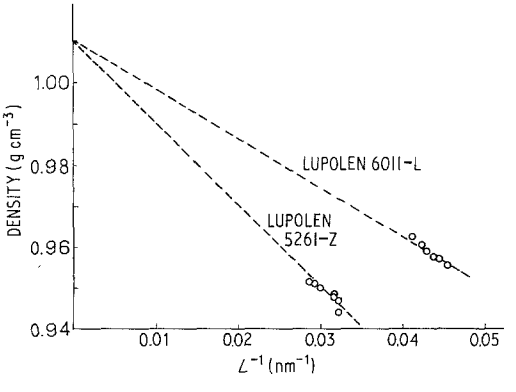

Figure 9 Plot of density (from Fig. 8) against L^{-1} (Fig. 7) for PE injection-moulded at different temperatures.

4. Discussion

Microhardness is a property sensitive to molecular orientation [2, 3]. Consequently, this technique offers an invaluable method for investigation of the structure of the molecular network of the solid moulded material. The SAXD results obtained for the high molecular weight polymer indicate the presence of a well-developed lamellar structure extending normal to the injection direction in the xy-plane. These lamellae contain a defective ("amorphous") surface layer of thickness about 12.5 nm, as inferred from the data of Fig. 9. The analysis of the broadening of the WAXD equatorial reveals, in addition, that the lamellae consist of blocks of dimensions approximately 50 nm. The blocks are reinforced by a great many tie molecules conferring to the material a large axial tensile strength and elastic modulus and contributing to the conspicuous elastic recovery of the indentation observed in the injection direction. In addition, the lateral grain boundaries of the blocks contain a multitude of chain segments which belong to the mobile three-dimensional molecular network connecting a great many blocks acting as knots of the said network. Fig. 10 is a schematic drawing of the structure of injection-moulded high molecular weight PE, which gives rise to an anisotropic indentation ($\Delta MH = 12\%$).

It has been previously pointed out [12, 16] that the structure of the molecular network in the melt can be transferred on cooling to the solid state. Since the deformation of the melt when filling up the mould cavity is admittedly given through the dimensions and geometry of the cavity, one would expect that the degree of molecular orientation achieved during moulding should, somehow, be related to the mesh density of the network in the molten polymer before injection. Accordingly, the finer the mesh of the three-dimensional network is, the higher the orientation of the network within the mould will be. Hence, since the hardness anisotropy of the plastic permanent impression arises from a local elastic recovery of oriented strands in the molecular direction, in our case the injection direction, one may anticipate that the mesh size of the molecular network will affect to a certain extent the elastic behaviour of the material beneath the indenter. The following observations are in favour of a correlation between microhardness and the structure of a molecular network in the injection moulded material:

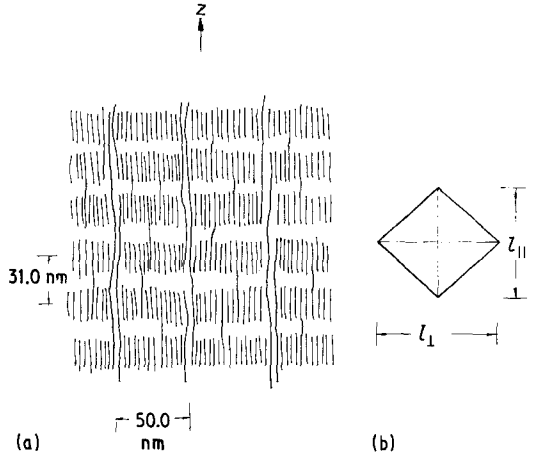

Figure 10 (a) Microstructure of injection-moulded high molecular weight PE. A lamellar structure with a periodicity of approximately 31.0 nm consisting of about 50.0 nm in lateral size is reinforced by a great many tie molecules parallel to the injection direction. The latter contribute to the elastic recovery of the material giving rise to (b) an anisotropic shape of Vickers indentation ($\Delta MH = 12\%$). The indentation diagonals are 10^3 times larger than the scale given for the microstructure.

(a) There is a sudden decrease of hardness anisotropy in the vicinity of 210° C, as shown in Fig. 3. Bayer and Ehrenstein [13] have shown that in this region a variation in the fracture mechanism of the moulded bars occurs. The mechanism is ductile above 210° C and brittle below this temperature. This transition in the mechanical properties of the mouldings has been interpreted in terms of a destruction of the molecular network above 210° C [13].

(b) The concurrent overall decrease of microhardness anisotropy for both molecular weight samples with increasing melt temperature within the injection moulder, T_s, suggests a decrease in the molecular network density (Fig. 3) with increasing T_s.

(c) Since the packing density of the molecular network depends on molecular weight it is not surprising that the value of ΔMH is substantially higher for Lupolen 5261-Z than for Lupolen 6011-L. This result is, furthermore, consistent with the fact that the former sample shows a good molecular and lamellar orientation (Fig. 4), respectively, parallel and perpendicular to the injection direction; the latter sample is characterized by a poor or absent orientation at both levels.

In conclusion, the above indications suggest that the hardness anisotropy depends directly on the nature of the molecular network of the material.

The remaining question is whether the role of

the molecular network may also influence the hardness value itself. From preceding studies on oriented chain-extended oriented PE [2] it is known that hardness itself is indeed an increasing function of crystal thickness and crystallinity [1]. The data of Figs 4 and 8 show, however, that L and the macroscopic density remain nearly unchanged with increasing T_s, implying that the thickness of the well-oriented lamellar structure is nearly independent of T_s. From Fig. 8 it may also be concluded that the crystallinity increases with T_w. The observed decrease of $MH_\perp$ and $MH_\parallel$ with T_s could be consequently associated with a worsening of interfibrilar connectedness and chain-packing in the injection direction giving rise, as a result, to a decrease of elastic properties and to a lower resistance to slippage of individual fibrils within the molecular network. The influence of the molecular network can be further illustrated by comparing the $MH_\perp$ data for the 6011-L and 5261-Z samples (Fig. 2). Thus, below 210° C, where the character of the network prevails, the $MH_\perp$ value of the sample with a lower molecular weight is notably smaller than that for the higher molecular weight system.

According to Bayer and Ehrenstein [12, 13], the mould temperature for the high molecular weight PE seems to be not so relevant to steering up the tensile mechanical properties of the injection-moulded samples. Figs 6, 7 and 8 reveal, nevertheless, for $T_w > 70°$ C, the concurrent increasing dependence of ΔMH, L and ρ on T_w for Lupolen 5261-Z. It is noteworthy that below 70° C the hardness orientation of the material is independent of both L and ρ. This suggests that in this range ΔMH is determined only by the elastic recovery of strands embedded within the molecular network structure irrespectively of lamellar thickness and perfection. Above 75° C, however, the thinner lamellae, (partly associated with a smaller lamellar periodicity contributing to the second SAXD scattering maximum [23]), cannot crystallize in the mould cavity. Above this temperature, one could expect a fractionation [24] of the lower molecular weight components giving rise to a better crystallization of the high molecular weight material. Hence, through the strain field developed within the molecular network during injection above 75° C, one could think of an improvement in the overall orientation of the moulded material. The orientation evidently increases, the greater is the contribution of material with higher molecular weight, that is the higher is T_w. Such a behaviour would demand the occurrence of a competition between a lamellar crystallization prevailing below 75° C against a developing strained molecular network structure predominating above 75° C. Evidence for a segregation of the high molecular material contributing to the molecular network during slow crystallization has been reported previously [17, 18]. In our case the molecular network is not so strong as to prevent crystallization, even at $T_w < 70°$ C.

The linear increase of $MH_\perp$ with T_w observed for Lupolen 6011-L (Fig. 5) cannot, anymore, be interpreted in terms of the molecular network concept. These mouldings do not show any molecular orientation whatsoever and only a weak lamellar orientation emerges for $T_s < 270°$ C. The material is isotropic and, therefore, no hardness anisotropy is detected. Hence, in analogy with preceding data on unoriented lamellar PE [5], the linear concurrent increases of MH, L and ρ with T_w (Figs 5, 7 and 8) imply that microhardness is therefore linearly correlated with lamellar thickness and overall density. Microhardness is thus mainly sensitive to the dimensions and perfection of the hard elements of the microstructure.

Finally, we wish to briefly comment on the conspicuous difference between the L values observed for Lupolen 5261-Z and Lupolen 6011-L for a given mould temperature (Fig. 7). This difference could be partly due to the influence of molecular weight on the unperturbed dimensions of the molecular coils in the liquid state [25]. These dimensions have been shown to be correlated to the long period [26]. In addition, the thermal treatment of these materials in the melt at T_s has presumably not been sufficiently long (20 to 30 sec) to erase the memory of the liquid state for the two samples which had independent thermal treatment and consequently different initial morphologies.

Acknowledgement

We wish to acknowledge the valuable help of Mr Jaime Garcia Peña in the microhardness measurements, and the Alexander von Humbolt Stiftung for generous support of this work.

References

1. F. J. BALTÁ CALLEJA, *Colloid Polymer Sci.* **254** (1976) 258.
2. F. J. BALTÁ CALLEJA and D. C. BASSETT, *J. Polymer Sci. Polymer Sym.* **58** (1977) 157.

3. F. J. BALTÁ CALLEJA, W. T. MEAD and R. S. PORTER, *Polymer Eng. Sci.* **20** (1980) 393.
4. F. J. BALTÁ CALLEJA, D. R. RUEDA, R. S. PORTER and W. T. MEAD, *J. Mater. Sci.* **15** (1980) 765.
5. F. J. BALTÁ CALLEJA, J. MARTINEZ SALAZAR, H. CACKOVIĆ and J. LOBODA-CACKOVIĆ, *ibid.* **16** (1981) 239.
6. A. PETERLIN, *ibid.* **6** (1971) 490.
7. J. MARTINEZ SALAZAR and F. J. BALTÁ CALLEJA, Proceedings of the IUPAC International Meeting on Macromolecules, Florence, September 1980, Paper 1C-49.
8. W. OWEN and D. HULL, *Plast. Polymer* **42** (1974) 19.
9. R. M. OGORKIEWICZ (Ed) "Thermoplastics" (Chemical Rubber Co., Cleveland, Ohio, 1969) p. 250.
10. R. L. BALLMAN, T. SHUSMAN and H. L. TOOR, *Mod. Plast.* (1959) 115.
11. J. L. WALKER and E. R. MARTIN, "Injection Moulding of Plastics" (Plastics Institute, Iliffe Books, London, 1966).
12. R. K. BAYER, *Colloid Polymer Sci.* **259** (1981) 303.
13. R. K. BAYER and G. W. EHRENSTEIN, *ibid.* **259** (1981) 293.
14. J. BOWMAN, N. HARRIS and M. BEVIS, *J. Mater. Sci.* **10** (1975) 63.
15. J. BOWMAN and M. BEVIS, *Colloid Polymer Sci.* **256** (1977) 954.
16. C. PICOT, R. DUPLESSIX, D. DECKER, H. BENOIT, F. BOUE, J. P. COTTON, M. DAOUD, B. FARNOUX, G. JANNINK, M. NIERLICH, A. J. DE VRIES and P. PINCUS, *Macromolecules* **10** (1977) 436.
17. G. CAPACCIO, T. A. CROMPTON and I. M. WARD, *J. Polymer Sci. Polymer Phys. Ed.* **14** (1976) 1641.
18. P. J. BARHAM and A. KELLER, *J. Mater. Sci.* **11** (1976) 27.
19. R. HOSEMANN, J. LOBODA-CACKOVIĆ and H. CACKOVIĆ, *Colloid Polymer Sci.* **254** (1976) 782.
20. E. W. FISCHER and G. F. SCHMIDT, *Angew. Chem.* **74** (1962) 551.
21. E. W. FISCHER, H. GODDAR and G. F. SCHMIDT, *J. Polymer Sci. Polymer Lett.* **5** (1967) 619.
22. G. T. DAVIS, J. J. WEEKS, G. M. MARTIN and R. K. EBY, *J. Appl. Phys.* **45** (1974) 4175.
23. J. MARTINEZ SALAZAR and F. J. BALTÁ CALLEJA, *Polymer Bull.* **3** (1980) 7.
24. J. DUGLOSZ, G. V. FRASER, D. GRUBB, A. KELLER, J. A. ODELL and P. L. GOGGIN, *Polymer* **17** (1976) 471.
25. J. RAULT and E. ROBELIN, *Polymer Bull.* **2** (1980) 373.
26. J. RAULT, *J. Macromol. Sci. Phys.* **B15** (1978) 567.

Received 12 March and accepted 20 May 1981.